SAND2022-12302C

Spectral Atmospheric Attenuating Effects for Heliostats and Receivers

Kenneth Armijo[1,a)], Nathan Schroeder[1], Aaron Rodriguez[1] and Aaron Overacker[1]

[1] Concentrating Solar Technology, Sandia National Laboratories, P.O. Box 5800, MS-1127, Albuquerque, NM 87185, USA

[a)] kmarmij@sandia.gov

1. Abstract

Site selection can have a large impact on the return on investment (ROI) for planned utility-scale concentrating solar power (CSP) plants. Site-specific solar spectrum must be considered to optimally utilize solar resources at a given location for a particular receiver and heliostat design. The reflectivity of heliostat mirror coatings as well as coatings for solar receivers can influence the overall heat absorption within heat transfer fluids (HTFs) and subsequent power production. The absorption of heat within particular infrared (IR) bands of the spectrum are also influenced by atmospheric aerosols which attenuate particular spectral bands from reaching the heliostat or receiver. These aerosols include water vapor, carbon-based aerosols (i.e. CO_2, CO, etc.), NO_2 and O_3. Since material spectral reflectivity and absorption for receivers and heliostats respectively can degrade over time, these spectral sensitivities can only increase, thus reducing power production. This investigation utilizes a custom spectrometer to collect spectral data during varying environmental conditions with these aerosols, by collecting data pointed at the sun and at a heliostat. The results suggest that higher humidity conditions reduced the overall round-trip flux to the receiver by approximately 24.4%. During smoky conditions solar energy flux was lost at more discrete, lower-wavelength bands due to CO_2, O_2, NO_2, and CO, where conditions with high PM 2.5 and PM10 values, the spectral irradiance absorbed in the receiver was less than for days with low levels of smoke, by as much as 9.4%.

Introduction

Concentrating solar power (CSP) design decisions pertaining to appropriate receiver design and heliostat field layout to optimize power generation for a respective site in turn can have a significant impact on ROI [1] for a given plant. For CSP tower technologies, ultimate energy absorption into the HTF within a receiver, and subsequent electric current generation is influenced by the spectral distribution of sunlight [2, 4] and its daily and seasonal variability, being impacted by radiation losses at the receiver, heliostat mirrors and air mass (AM). According to Bird *et al.* [5], within the atmosphere, photons can undergo scattering from air molecules (Rayleigh scattering) and suspended particulate matter (aerosol scattering), absorption by molecules or aerosols, and reflections from the ground, Fig. 1.

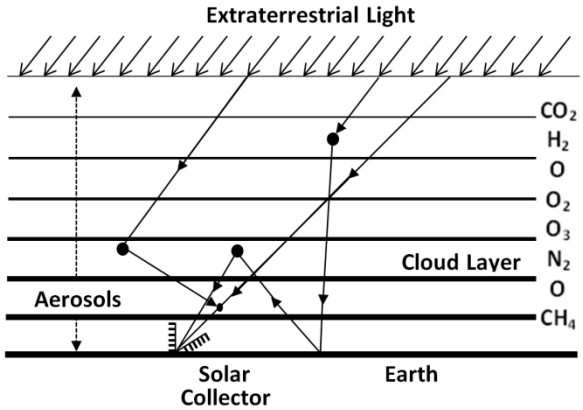

Figure 1. Radiative transfer model by Bird et al. [5] with absorbing atmospheric constituents.

To illustrate the pronounced impacts of atmospheric aerosols and air mass on spectral attenuation, research by Litjens [6] (Fig. 2) showed that as air mass (AM) and aerosol optical depth (AOD) increase, irradiance in shorter wavelengths (280-1000 nm) decrease faster than at longer wavelengths. This occurs since photons with shorter wavelengths facilitate scattering at lower wavelengths compared with those that are longer. Also, precipitable water absorption bands located at 1500, 2000, and 2500 nm decrease to zero from 0-0.5 atm-cm, while ozone is shown to only have a small effect in the wavelengths between 350-800 nm.

Unlike photovoltaic (PV) systems where the potential for spectral atmospheric attenuation due to aerosols [7] is only between the sun and the module normal, attenuation in CSP tower facilitates can be found also between the heliostats and the tower receiver. For heliostat fields that can be larger than a few kilometers in diameter [8,9,10], these atmospheric attenuation losses can also be significant. Additionally, CSP plants aerosol concentrations of smoke from forest fires or smog, as well as humidity, can have a notable impact on

the integrated solar direct normal irradiance (DNI) resource potential. Additionally, the scale of influence changing spectrum can have on CSP receiver performance may vary significantly depending on the receiver absorber coating and heliostat mirror composition/coatings being employed. However, spectral variability introduces a systematic influence on performance that is dependent on time-of-day, season and location [11] that ideally should be accounted for.

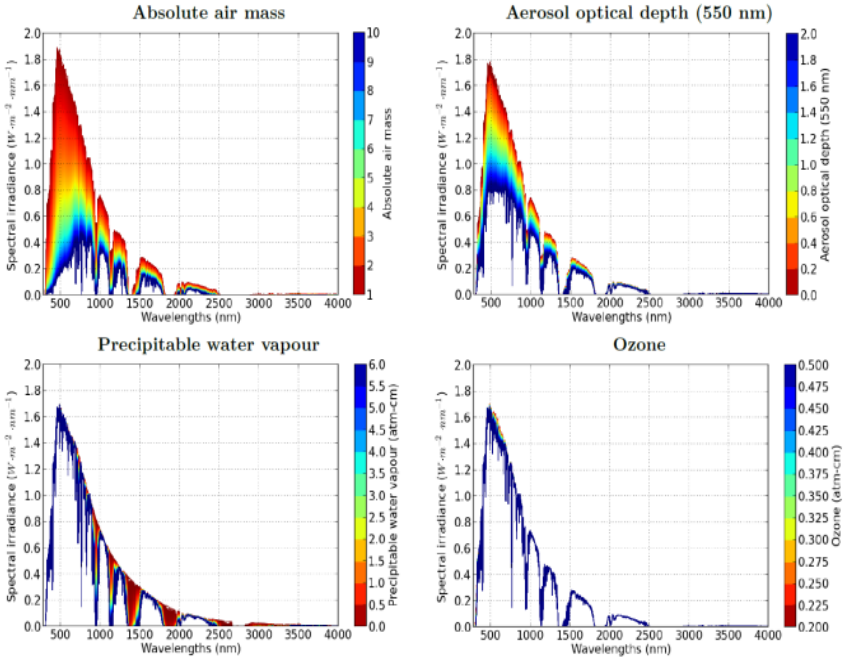

Figure 2. Effect of influencing parameters on spectral irradiance [6].

In CSP systems both the receiver and heliostat mirrors can be impacted by alternation of the solar absorption and reflectivity as a function of degradation and mirror soiling respectively. These localized derate factors in addition to atmospheric attenuation can ultimately decrease the level of heat transmitted to the receiver working fluid [12]. Assessment of the longitudinal reliability changes of the receiver and heliostats, convolved with the atmospheric spectral derates as a function of aerosol composition is important to manage the economic efficiency of a plant, as well as to plan for operation and maintenance [13]. Previous research by Henrieder et al. [14] evaluated various applied model equations and found that the effect of atmospheric aerosols attenuation can account for a reduction of annual plant yield of up to 18.2% and is dependent on the heliostat field size, the operational strategy, as well as the on-site atmospheric conditions. Site dependent models have been developed that have previously characterized aerosol optical depth (AOD) [15] and with respect specifically to relative humidity [16]. Site-specific models assessing atmospheric composition for varying aerosols, have been assessed within look-up tables (LUT) to determine an extinction range, though based on vertical profile assumptions.

Few models to date have considered the complex interplay between aerosol atmospheric attenuation with respective heliostat and receiver spectral losses. In this paper the team presents an approach for assessing the spectral energy derates associated with CSP systems. Experimental measurements were taken using a custom spectrometer [1] that was able to recreate the spectrum within less than 1% RMS error. The team collected data over a five-month period to assess spectral energy losses primarily due to smoke and humidity where data was collected near solar noon. The team also convolved mirror and receiver reflectivity data to assess conjugate losses with respect to mirror soiling and receiver coating degradation. The receivers evaluated were from solar pilot systems that included molten salt as the HTF [17,18,19].

2. Spectral Analysis Setup

The test setup included a small solar spectrometer mounted to the top of the Sandia National Laboratories (SNL), National Solar Thermal Test Facility (NSTTF), at a height of approximately 200 ft. with a solar spectrometer sight assembly, mounted for precision solar tracking. The team used a custom spectrometer (Fig. 3) developed by SNL [1]. The spectrometer was mounted on a solar tracker so it could continuously be positioned normal to the sun. The spectrometer was built as a low-cost device [1], consisting of six discrete bands that can be convolved together utilizing an algorithm by Tatsiankou et al. [19] to recreate the spectrum

to within +/- 5% error. The team performed several experiments collecting data within +/- 1 hr. from solar noon between March and June 2022.

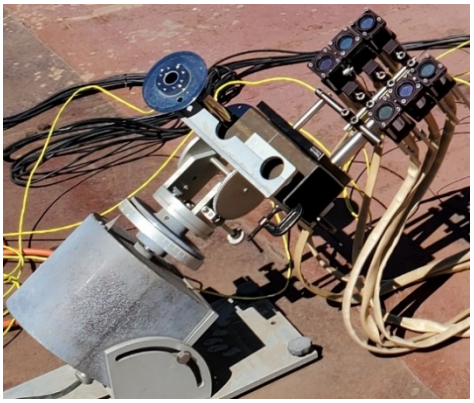

Figure 3. Custom 6-Band SNL Spectrometer.

A National Instruments (NI) data acquisition (DAQ) was used to collected data within 1 Hz frequencies where a time averaging was conducted over the 30 seconds data collection duration. Receiver coating and heliostat reflectance was measured using a handheld Solar 410 SOC reflectometer (Surface Optics, Model# 0410-0004) which measured the solar-weighted reflectivity of a surface in 6 spectral bands between 0.30-2.5 μm, Fig. 4.

a.  **b.** 

Figure 4. SOC Reflectometry for a. NSTTF heliostat mirror, and b. CSP receiver.

The device features a circular measurement aperture of 1.3 cm with the source of the measured reflection oriented 20° from normal. Total solar absorptance was obtained by subtracting the total solar hemispherical reflectance from one. To take the measurement, the Solar 410 aperture was positioned on the surface, and three individual measurements were taken. The three measurements were averaged, and the standard deviation between the measurements was recorded.

3. Analysis & Discussion

Spectral data was collected from the top of the solar tower using the customer spectrometer, which tracked the sun +/- 1 hr. from solar noon on the respective experimental evaluation days. Specific dates were chosen with respect to clear, smokey (from nearby forest fires) and relatively humid days (day after rainstorms) to be compared with regards to spectral irradiance. This data was also convolved with U.S. EPA air-quality index data to identify the smokiest and most humid days of the months while having direct normal irradiance (DNI) values above 900 W/m^2, which is the typical threshold considered for CSP receiver evaluation at the NSTTF. Comparisons of the results between humid and respective clear sky days for the same month, indicated that humidity impacted the overall spectrum more so than for smokey days. As shown in Fig. 5, the average values for smokey and humid days were found to be less than the average clear sky days by an average wavelength difference of 13.7% and 35.2% respectively.

For days with relative humidity (RH) as high as 42.8% and 67.9%, the average deviation as compared to a clear sky day was found to be 3.6% and 59.6% respectively. Additionally, during the same the same four-month evaluation period, particulate matter (PM) 2.5 and PM 10 data was collected for days based on relative level of haze while still not having any clouds present. For a 107 PM2.5 and 298 PM10 the average spectral irradiance deviation from a clear sky day was found to be 9.4%. spectral irradiance on different weather days.

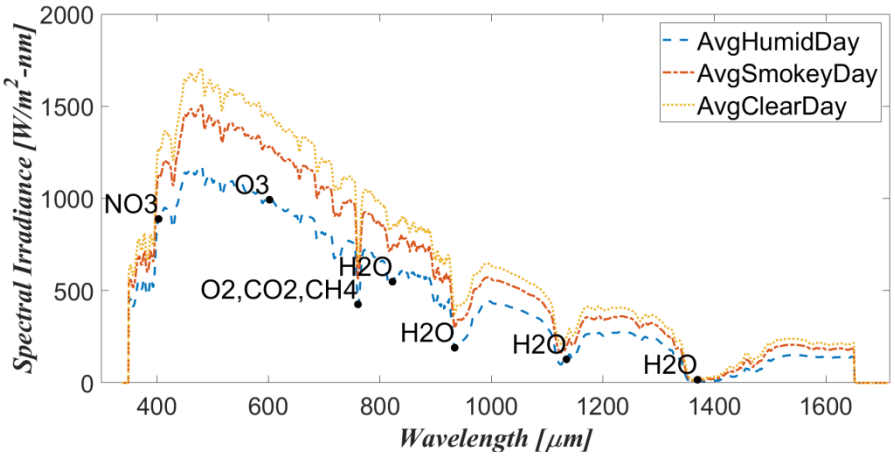

Figure 5. Average spectral irradiance data from different weather days being clear sky days, humid days, and smoky days with corresponding transmissivity band peaks.

The spectral irradiance for clear sky days was consistently higher due to aerosol particles preferentially absorbing energy within varying spectral bandwidths, which subsequently affects the transmissivity of energy passing from the sun to the CSP receiver. Transmissivity data for various atmospheric aerosols is presented by Fig. 6 by Tatsiankou et al. [19], which shows the high attenuation from water across the wavelengths of interest for this investigation, between 350-1,700 µm. Transmission for methane (CH_4), carbon dioxide (CO_2) and Oxygen (O_2) and nitrogen (N_2) was found to have less attenuation, though with impacts at more discrete bandwidths, though with more pronounced effects during smokey days.

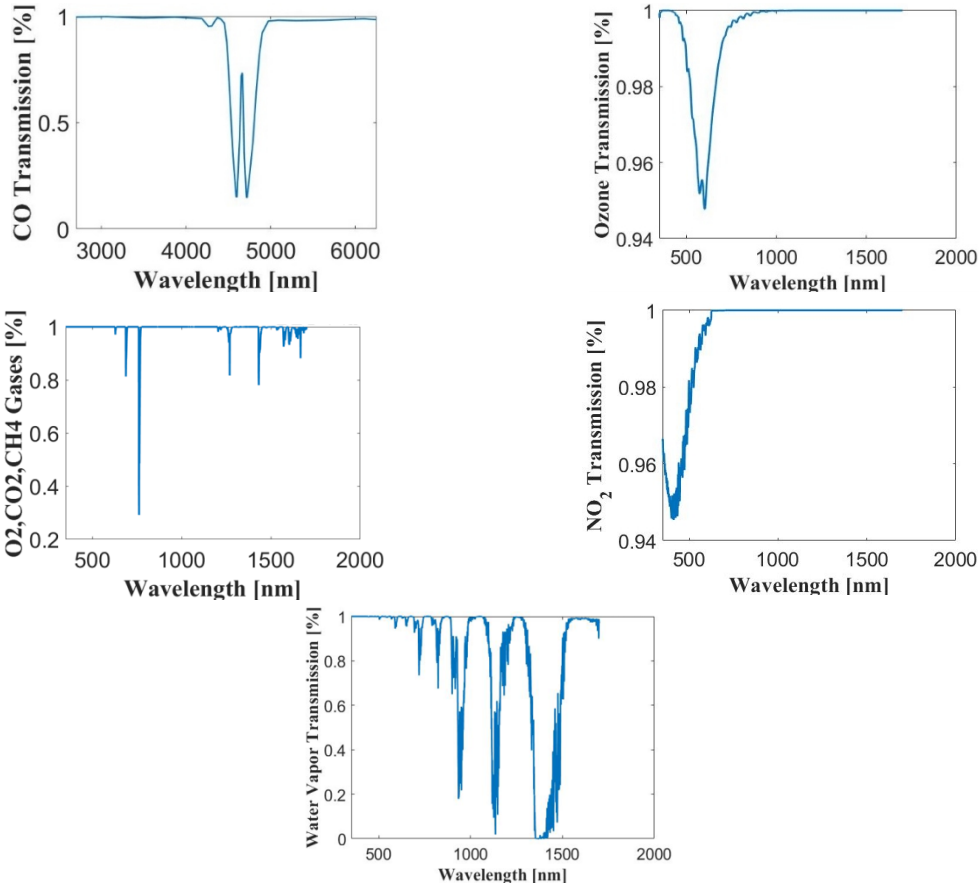

Figure 6. Carbon Monoxide (CO), Ozone (O_3), Oxygen (O_2), Methane (CH_4), Nitrogen Dioxide (NO_2) transmissivity percentages [19] showing the attenuation of wavelength where this air particle masses are being absorbed.

Assessment of the total transmitted energy also requires consideration for the losses at, and between the heliostats mirror surfaces and receiver tubes. Many heliostat mirrors often have a reflectance of approximately 92-97% when clean [20,21] though can have increased reflection losses up to 25% due to soiling

[22]. Table 1 provides the absorptance values obtained for the receiver tubes sets 1 and 2, which determined integrated reflectance values of 317.1 and 1226.2 respectively. Table 2 provides measured spectral reflectance values from a representative clean and a soiled heliostat at the SNL NSTTF. The integrated reflectivity values from clean and soiled heliostats were found to be 1289.1 and 1219.8 respectively.

Sample	335-380nm	400-540nm	480-600nm	590-720nm	700-1100nm	1000-1700nm
Receiving Tubes 1	0.961	0.960	0.961	0.960	0.958	0.952
Receiving Tubes 2	0.897	0.897	0.895	0.891	0.855	0.877

Table 1. Absorptivity for Investigated Receiver Tubes

Sample	335-380nm	400-540nm	480-600nm	590-720nm	700-1100nm	1000-1700nm
Clean Heliostat	0.809	0.940	0.953	0.955	0.938	0.961
Soiled Heliostat	0.788	0.929	0.942	0.946	0.932	0.956

Table 2. Reflectivity for a clean and soiled heliostat after snowing

To holistically characterize radiative losses from the sun to the receiver, analysis was performed to assess spectral losses that include reflectance losses from the heliostat (for a clean and soiled mirror surface) for two different receiver tubes. As shown in Fig. 7 the heliostat and receiver tubes (sets 1 and 2) reflectance losses were factored into the averaged data for a clear sky day the two sets of receiver tubes had varying levels of operational degradation per the reflectance measurements provided against the right axes of the figure, and as prescribed in the convolved losses. The results indicated that the soiled heliostat and the set 2 receiver tubes, which had more environmental wear, had greater reflectance losses from that of the clean heliostat and first set of receiver tubes respectively. The results also indicate that spectrally, the reflectance losses for the clean and soiled heliostats were more pronounced for wavelengths less than 485 nm. Which is approximately where the highest non-dimensional irradiance intensity deviations were found.

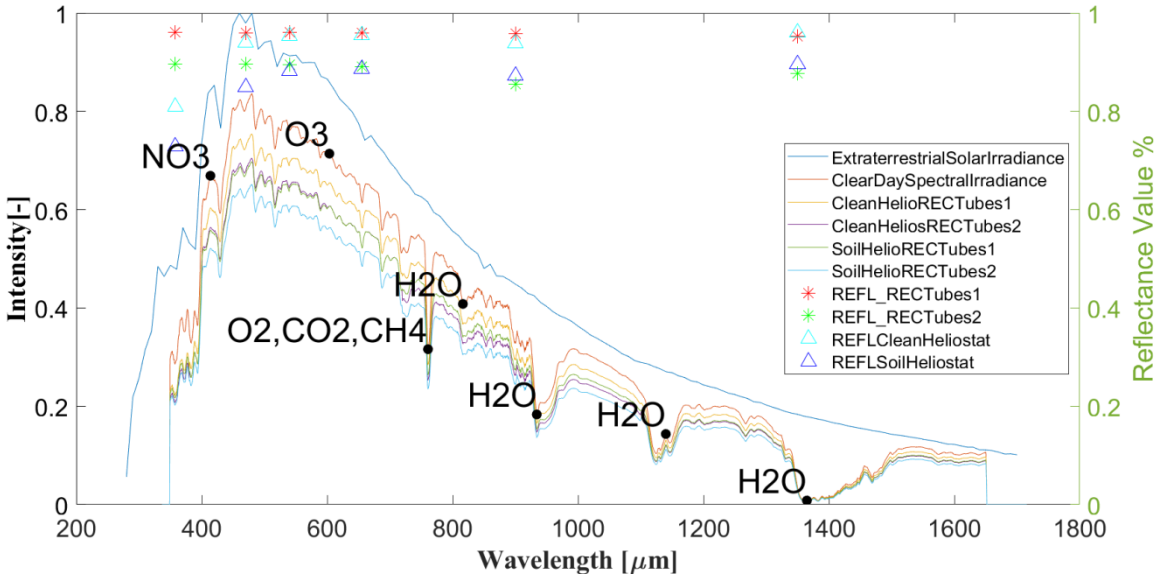

Figure 7. Comparison of spectral irradiance from extraterrestrial, attribution of average of *dry, clear sky days*, reflectivity from clean and soiled heliostats to receiver tube sets 1 and 2, and transmissivity reduction peaks for selected aerosols.

To assess spectral losses more graphically, Fig. 8 provides a Sankey diagram with corresponding knockdown values for a dry, non-smokey clear sky day, from extraterrestrial spectral irradiance (AM 0, [5]) to the average of the dry, clear sky days data. Here, the results suggest a 26% heat flux loss only due to aerosol attenuation, while reflectance losses due to a clean and soiled heliostat found 30% 35% total losses respectively. Total

reflectivity losses from the receiver tubes was found to be 9.1% for an overall 55.88% total heat flux which can be transferred to a respective HTF.

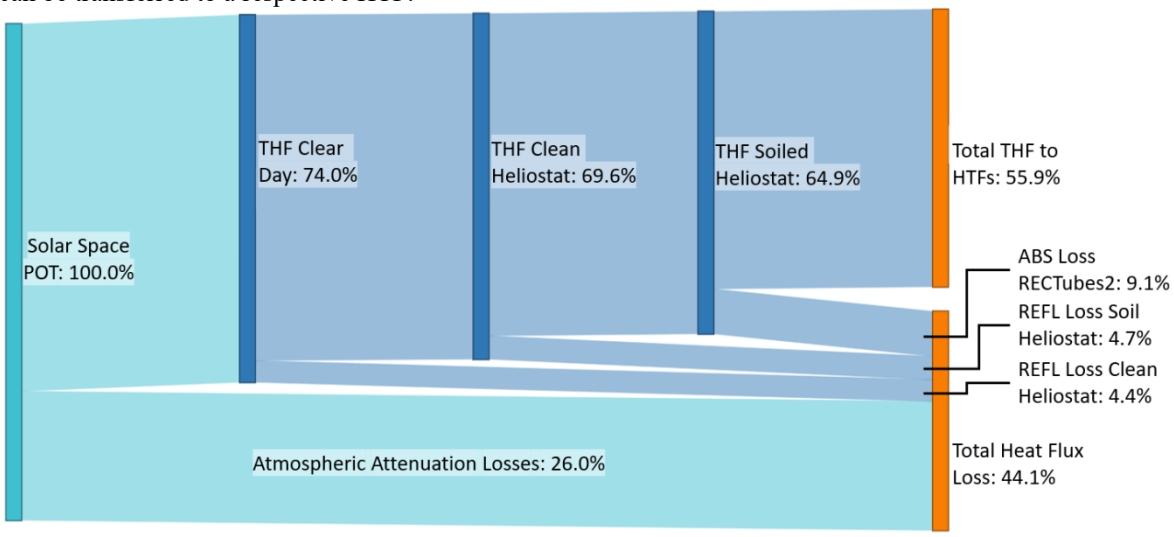

Figure 8. Sankey diagram for transfer heat flux (THF) to receiver and heat flux losses during *dry, clear sky days*.

For days with humidity, results shown in Fig. 9 suggested the knockdown factor from the extraterrestrial spectral irradiance to the averaged measured spectral irradiance was approximately 49%. When the reflectivity losses were factored in for a clean and soiled heliostat, the total losses were found to be 53% and 56% respectively. The final absorptivity to the receiver tubes 2 was found to be approximately 39%. Therefore, in comparison to a dry, clear day, the final overall flux was reduced by approximately 24.4%.

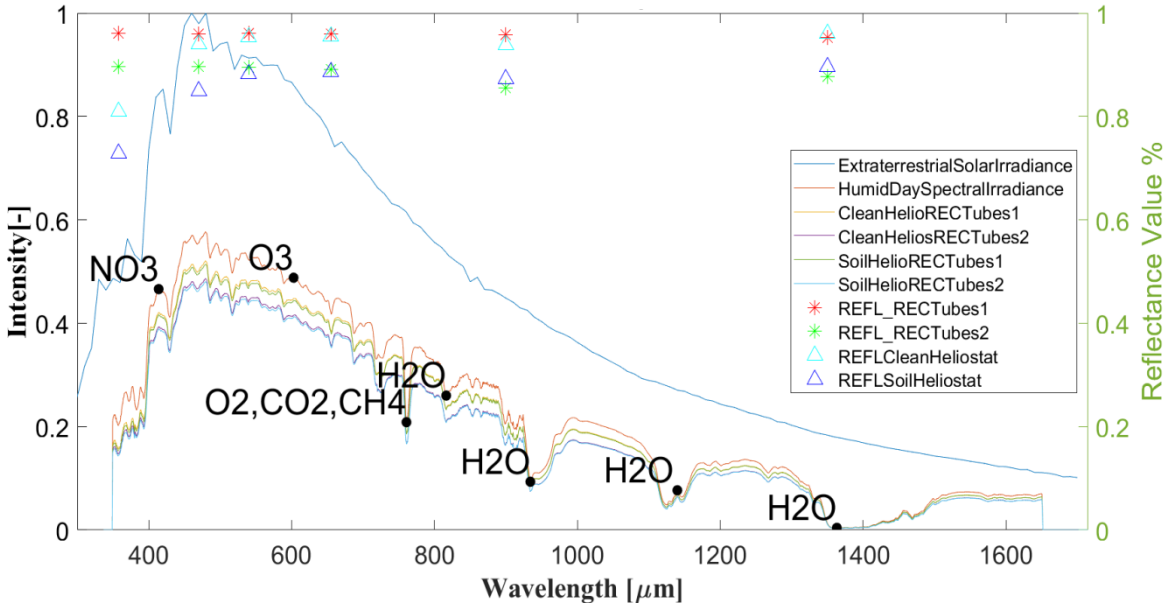

Figure 9. Comparison of spectral irradiance from extraterrestrial, attribution of a *humid day*, reflectivity from clean and soiled heliostats to receiver tube sets 1 and 2, and transmissivity reduction peaks for selected aerosols including H_2O.

The sanky diagram pertaining to humid conditions is presented in Fig. 10 which presents a total atmospheric attenuation of 50.3%. When the reflectivity losses from the heliostat and receiver tubes were factored into the total heat flux for the HTF was found to be 38.8% with a respective total heat flux loss of 61.2%. However, depending on the time of year and day, these losses could differ further, requiring further data collection and analysis over other seasons and relative humidity conditions.

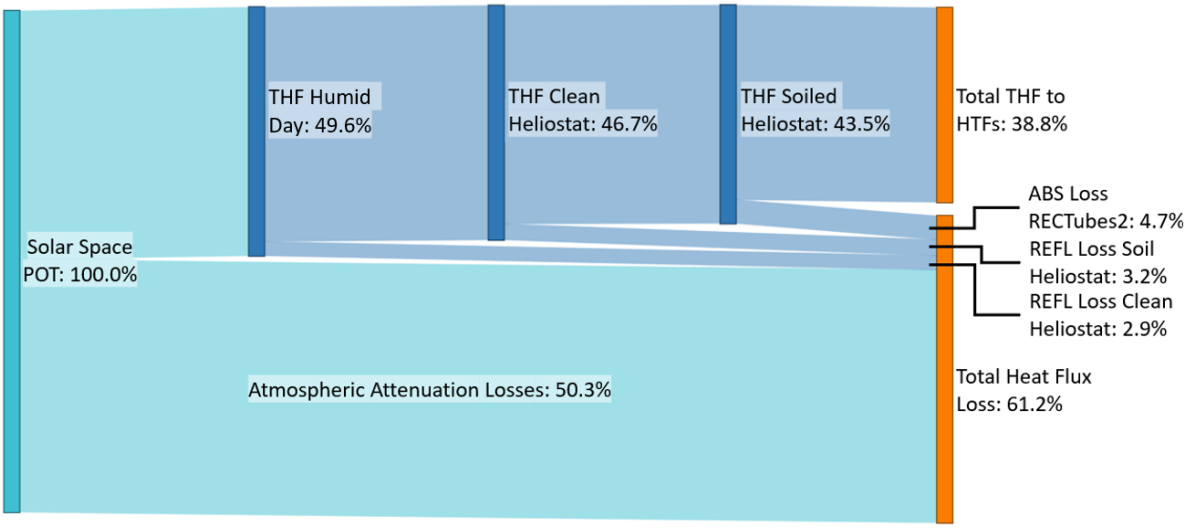

Figure 10. Sankey diagram for transfer heat flux (THF) to receiver and heat flux losses for days with relatively high *humidity*.

Finally, for days with smokey weather conditions, the averaged convolved spectral irradiance results, Fig. 11, shows higher overall non-dimensionalized irradiance values compared to humid days. This was due to water vapor absorbing more within the three longer-wave IR bands. During smokey days however flux was lost at more discrete, lower-wavelength bands due to CO_2, O_2, NO_2, and CO. One should note however from Fig. 6, CO is mostly absorbed at much higher wavelengths in the far infrared spectrum.

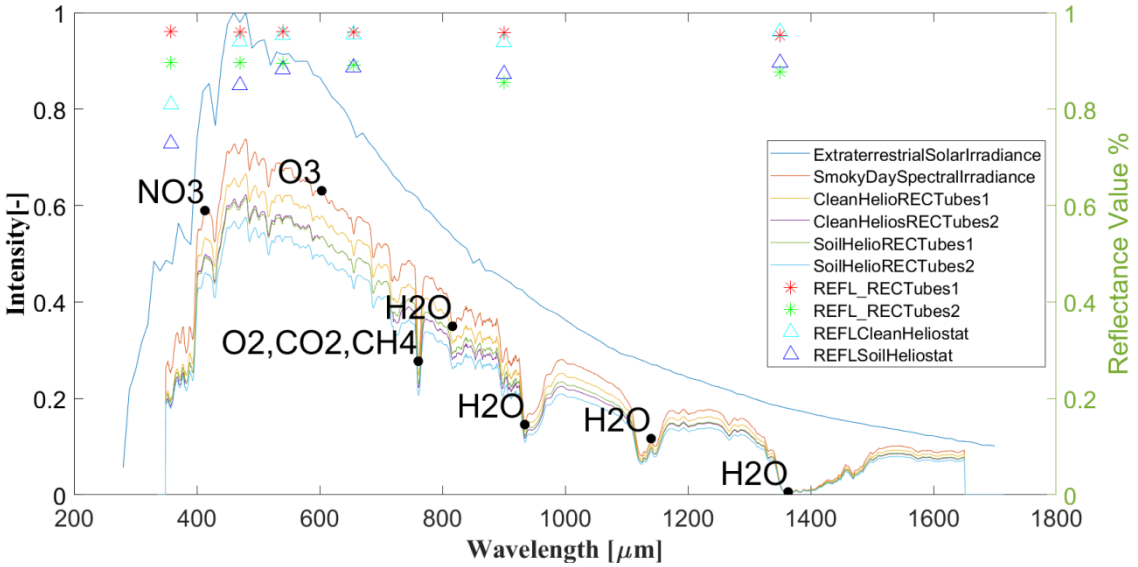

Figure 11. Comparison of spectral irradiance from extraterrestrial, attribution of an average of *smoky days*, reflectivity from a clean and soiled heliostats to receiver tubes 1 and 2, and presenting transmissivity reduction peaks for mixed gases of O_2, CO_2, CH_4, NO_2 and CO.

From the Fig. 12 results, the knockdown losses from extraterrestrial spectral irradiance for the averaged days under smokey conditions was 35%. Accounting for reflectivity losses, a clean heliostat had 39%, a soiled heliostat had 43% and the receiver tubes 2 had 49%, making the total heat flux going into the receiver 50.65%. The results therefore indicate that days with high PM 2.5 and PM10 values, the spectral irradiance absorbed in the receiver was less than for days with low levels of smoke, by as much as 9.4%.

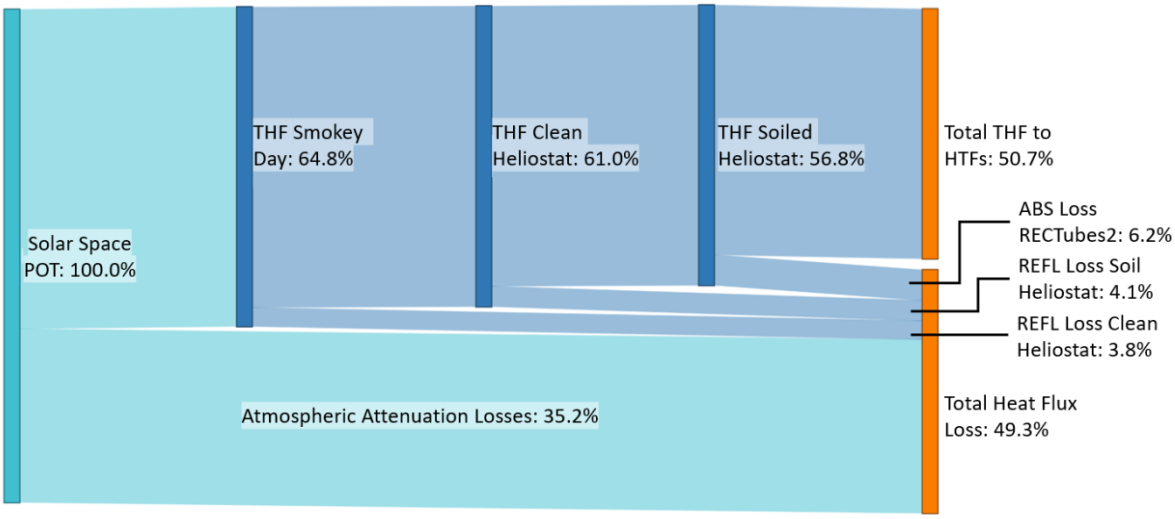

Figure 12. Sankey diagram for transfer heat flux (THF) to reciever and heat flux losses in during *smoky* weather conditions.

4. Conclusion

A spectral attenuation investigation was performed to assess the impacts of atmospheric components in the atmosphere as a function of air mass and reflected light from heliostats that are positioned in front of CSP receivers. Data was collected during dry, clear sky and smokey weather conditions, and convolved with measured reflectivity values of clean and soiled heliostats as well as two CSP receivers. The results indicated that the soiled heliostat and the set 2 receiver tubes, which had more environmental wear, had greater reflectance losses from that of the clean heliostat and first set of receiver tubes respectively. The results also indicate that spectrally, the reflectance losses for the clean and soiled heliostats were more pronounced for wavelengths less than 485 nm. The convolved spectral results suggest for a dry, clear sky day a 26% heat flux loss only due to ambient aerosol attenuation, while reflectance losses due to a clean and soiled heliostat found 30% 35% total losses respectively. Total reflectivity losses from the receiver tubes were found to be 9.1% for an overall 55.88% total heat flux which can be transferred to a respective HTF. With higher humidity conditions the overall round-trip flux to the receiver was reduced by approximately 24.4%. During smokey conditions solar energy flux was lost at more discrete, lower-wavelength bands due to CO_2, O_2, NO_2, and CO, where conditions with high PM 2.5 and PM10 values, the spectral irradiance absorbed in the receiver was less than for days with low levels of smoke, by as much as 9.4%.

5. Acknowledgements

Sandia National Laboratories is a multimission laboratory managed and operated by National Technology and Engineering Solutions of Sandia, LLC., a wholly owned subsidiary of Honeywell International, Inc., for the U.S. Department of Energy's National Nuclear Security Administration under contract DE-NA0003525. The team would also like to acknowledge the support from the U.S. DOE Solar Energy Technologies Office (SETO) as well as contributions from the U.S. Air Force Nuclear Weapons Center (AFNWC) for this research.

References

[1] K.M. Armijo and J. Yellowhair, Sandia National Laboratories, SAND2014-19826, 2014.
[2] Tatsiankou, V., Hinzer, K., Mohammed, J., Muron, A., Wilkins, M., Haysom, J., Schriemer, H. and Myrskog, S., Photonics North, Vol. 8915, pp. 33-43, SPIE, 2013.
[3] King, D.L., Kratochvil, J.A. and Boyson, W.E., "Measuring solar spectral and angle-of-incidence effects on photovoltaic modules and solar irradiance sensors," 26th IEEE PVSC Conference, Anaheim, CA, 1997.
[4] A. Feltrin and A. Freundlich, "Material considerations for terawatt level deployment of photovoltaics," J. Renewable Energy, 33, no. 2, pp. 180-185, 2008.
[5] R.E. Bird, R.L. Hulstrom, "Terrestrial solar spectral data sets," Solar Energy, 30, No. 3, pp. 563-573, 1993.
[6] G.B. Litjens, "Investigation of Spectral Effects on Photovoltaic Technologies by Modelling the Solar Spectral Distribution." Master's Thesis, Universiteit Utrecht, 2013.

[7] Armijo, K.M., Harrison, R.K., King, B.H. and Martin, J.B., "Spectral derates phenomena of atmospheric components on multi-junction CPV technologies," AIP Conference Proceedings, Vol. 1616, No. 1, pp. 264-271, 2014.
[8] Zhang, H., Benoit, H., Perez-Lopèz, I., Flamant, G., Tan, T. and Baeyens, J., "High-efficiency solar power towers using particle suspensions as heat carrier in the receiver and in the thermal energy storage," Renewable Energy, 111, pp.438-446, 2017.
[9] Collado, F.J. and Guallar, J., "A review of optimized design layouts for solar power tower plants with campo code," Renewable and Sustainable Energy Reviews, 20, pp.142-154, 2013.
[10]. Merchán, R.P., Santos, M.J., Medina, A. and Hernández, A.C., "High temperature central tower plants for concentrated solar power: 2021 overview," Ren. & Sus. Energy Reviews, p.111828, 2021.
[11] I.B. Karki and D. Faiman, "Solar spectral influence on the performance of crystalline based photovoltaic modules under hot weather conditions," Scientific World, 11, no. 11, pp. 48-51, 2013.
[12] Reoyo-Prats, R., Plaza, A.C., Faugeroux, O., Claudet, B., Soum-Glaude, A., Hildebrandt, C., Binyamin, Y., Agüero, A. and Meißner, T., "Accelerated aging of absorber coatings for CSP receivers under real high solar flux–Evolution of their optical properties," Solar Energy Materials and Solar Cells, 193, pp.92-100, 2019.
[13] A. Boubault, K.C. Ho, A. Hall, T.N. Lambert, A. Ambrosini, "Durability of solar absorber coatings and their cost-effectiveness," Sol. Energy Mater. Sol. Cells 166, 176–184, 2017.
[14] Hanrieder, N., Wilbert, S., Mancera-Guevara, D., Buck, R., Giuliano, S. and Pitz-Paal, R., "Atmospheric extinction in solar tower plants–A review," Solar Energy, 152, pp.193-207, 2017.
[15] Polo, J., Ballestrín, J., Carra, E., "Sensitivity study for modelling atmospheric attenuation of solar radiation with radiative transfer models and the impact in solar tower plant production," Solar Energy 134, 219–227, 2016.
[16] Hanrieder, N., Ghennioui, A., Wilbert, S., Sengupta, M. and Zarzalejo, L.F., "AATTENUATION—The Atmospheric Attenuation Model for CSP Tower Plants: A Look-Up Table for Operational Implementation," Energies, 13(20), p.5248, 2020.
[17] Smith, D.C. and Chavez, J.M., "A final report on the Phase I testing of a molten-salt cavity receiver: Volume 1, A summary report," SAND87-2290, Sandia National Laboratories, 1988.
[18] Prairie, M.R., Pacheco, J.E., Gilbert, R.L., Reilly, H.E., Speidel, P.J. and Kelly, B.D., "Performance of the solar two central receiver power plant," SAND-97-3196C, Sandia National Laboratories, 1998.
[19] Tatsiankou V, Hinzer K, Mohammed J, Muron A, Wilkins M, Haysom J, Schriemer H, Myrskog S. "Reconstruction of solar spectral resource using limited spectral sampling for concentrating photovoltaic systems," SPIE Photonics North, Vol. 8915, pp. 33-43, 2014.
[20] Sarasua, J.A., Sandá, A., Villasante, C. and Aranzabe, E., "Non-immersion ultrasonic cleaning for heliostats," AIP Conference Proceedings, Vol. 2033, No. 1, p. 040035, 2018.
[21] King, D.L. and Myers, J.E., "Environmental reflectance degradation of central receiver test facility (CRTF) heliostats," In Optics in Adverse Environments II, Vol. 216, pp. 255-261, SPIE, 1980.
[22] Berg, R.S., "Heliostat dust buildup and cleaning studies" SAND78-0510, Sandia National Laboratories, 1978.